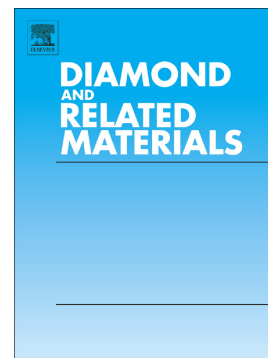


© <2020>. This manuscript version is made available under the CC-BY-NC-ND 4.0 license
<http://creativecommons.org/licenses/by-nc-nd/4.0/>
The definitive publisher version is available online at <https://doi.org/10.1016/j.diamond.2020.108081>

Zr(IV) functionalized Graphene oxide anchored sand as potential and economic adsorbent for fluoride removal from water

C. Prathibha, Anjana Biswas, L.A. Avinash Chunduri, Shiva Konda Reddy, Paripurnanda Loganathan, Mahatheva Kalaruban, Kamiseti Venkatarmaniah



PII: S0925-9635(20)30634-8

DOI: <https://doi.org/10.1016/j.diamond.2020.108081>

Reference: DIAMAT 108081

To appear in: *Diamond & Related Materials*

Received date: 25 June 2020

Revised date: 19 August 2020

Accepted date: 3 September 2020

Please cite this article as: C. Prathibha, A. Biswas, L.A.A. Chunduri, et al., Zr(IV) functionalized Graphene oxide anchored sand as potential and economic adsorbent for fluoride removal from water, *Diamond & Related Materials* (2020), <https://doi.org/10.1016/j.diamond.2020.108081>

This is a PDF file of an article that has undergone enhancements after acceptance, such as the addition of a cover page and metadata, and formatting for readability, but it is not yet the definitive version of record. This version will undergo additional copyediting, typesetting and review before it is published in its final form, but we are providing this version to give early visibility of the article. Please note that, during the production process, errors may be discovered which could affect the content, and all legal disclaimers that apply to the journal pertain.

**Zr(IV) functionalized Graphene oxide anchored sand as potential and economic adsorbent
for fluoride removal from water**

C. Prathibha^{a*}, Anjana Biswas^a, L. A. Avinash Chunduri^a, Shiva Konda Reddy^b, Paripurnanda
Loganathan^c, Mahatheva Kalaruban^c and Kamiseti Venkatarmaniah^a

^a *Laboratories for Nanoscience and Nanotechnology Research, Department of Physics, Sri
Sathya Sai Institute of Higher Learning, Prasanthinilayam, 515134, A.P. India*

^b *Faculty of Engineering, Jawaharlal Nehru Technology University, Hyderabad, A.P. India*

^c *Faculty of Engineering and Information Technology, University of Technology, Sydney, NSW,
2007, Australia*

^{a*}Corresponding Author: Dr.C.Prathibha
Assistant Professor
Sri Sathya Sai Institute of Higher Learning
Andhra Pradesh, India
mob: +91 9490362024
mail: cprathibha@sssihl.edu.in

Abstract

Excessive fluoride (F) in drinking water is a major problem affecting human health in many parts of the world. Cost-effective adsorbents are required for the defluoridation of drinking water. A carbon-based adsorbent, graphene oxide coated sand was produced from very inexpensive materials, sugar and river sand and impregnated with zirconium (Zr) for defluoridation of water. F adsorption by Zr impregnated graphene oxide coated sand (ZIGCS) at pH 4.0 satisfactorily fitted to Langmuir and Freundlich adsorption models with a Langmuir maximum adsorption capacity of 6.12 mg/g which is one of the highest values among the other carbon-based economic adsorbents reported for defluoridation. The adsorption of F on to ZIGCS (point of zero charge of pH 4.5) increased from pH 2 to 4 and then decreased up to 12. However, considerable adsorption capacity was observed throughout this pH range. Pseudo-second order model successfully described the adsorption reaction kinetics. Fluoride adsorbed on to ZIGCS was effectively desorbed using 0.1 M NaOH and the regenerated adsorbent maintained approximately 75% of the original F adsorption capacity even after five regeneration cycles. Thermodynamic data revealed that the adsorption process was endothermic and spontaneous with increase in randomness at the solid/solution interface.

Highlights

1. ZIGCS, a product of Zirconium Impregnated Graphene oxide, anchored on Sand is a low cost adsorbent for defluoridation of water
2. The adsorbent is produced from inexpensive materials: table sugar and sand
3. Quick and rapid Removal of fluoride is possible with ZIGCS
4. It could retain 75% of its F⁻ removal capacity even after five regeneration cycles

Keywords: adsorption, defluoridation, fluoride, graphene oxide, zirconium impregnated graphene oxide.

1. Introduction

Fluoride (F) contamination of drinking water has been recognised as one of the major problems in the global context due to its adverse effects on human health [1][2]. Depending on the amount present in water, F is both tonic and toxic in nature. It is treated as an important mineral for protection against dental carries at lower concentrations below 1 mg/L. On the contrary, when it exceeds 1.5 mg/L it leads to serious health hazards such as skeletal and dental fluorosis. As per the World Health Organization standards [3] the maximum permissible F concentration in drinking water is 1.5 mg/L. In many parts of the world, F in groundwater used for drinking exceeds 1.5 mg/L. Hence, knowledge of its removal, using a viable technique with high efficiency is most needed. Among various techniques available, adsorption is the most suitable and extensively used technique due to its simple operation and the low cost involved.

Carbon has been the most versatile material used for water purification in history. Very early account of the use of charcoal in water purification is found in the Vedic literature. It is believed, people of Indus valley civilization used carbon and porous materials, such as earthen vessels, for filtering and storing drinking water. Today, carbon has become one of the most common and trusted material for water remediation [4]. Activated carbons[5] derived from various plant sources have been widely used as adsorbents in water treatment. Carbon based nanomaterials have fascinated the entire scientific community by their unique physiochemical properties and wide range of applications. After the discovery of fullerene and carbon nanotubes (CNTs), research has been focused on another allotrope of carbon, and its derivatives. Graphene and its derivatives (graphene oxide (GO), reduced graphene oxide (rGO)) are among attractive newly emerging additions into the carbon family[6]. It is a carbon allotrope that has attracted immense research in recent years. Graphene is a two-dimensional nanomaterial that has one to ten layers of sp^2 -hybridized carbon atoms arranged in six-membered rings; whereas GO has similar structure but with many oxygen based functional groups like hydroxyl ($-OH$), alkoxy ($C-$

O–C), carbonyl (C = O), carboxylic acid (–COOH) [7,8]. Therefore, various kinds of defects are brought into the (vacancy defect, hole defect) inert structure of graphene by means of the oxygen functionalization present in GO structure. Defect rich structures such as these gives rise to many unique properties in GO which makes it available for various applications[6][9]. Hence GO has a backbone of graphene's electron-rich π – system [10] and electron rich oxygen species [11]. Graphene possesses a large theoretical surface area (2630 m²/g) [12] and that of graphene oxide in water was calculated to be 2418 m²/g [13]. These properties make GO a potential revolutionary adsorbent for environmental pollutant management.

However, there seems to be not much work done in exploring pure graphene as an efficient adsorbent of F except the work of Li et al. (2011) [14] who studied the capacities and rates of F adsorption onto graphene at different initial pH and temperature. They reported a Langmuir adsorption capacity of 35.59 mg F/g at pH = 7.0 and at 298 K for the graphene which was shown to be among the highest adsorption capacities recorded for F. However, there are numerous challenges to be faced in using graphene based materials (graphene, GO, rGO) alone as an adsorbent. The first is their high cost. Therefore, it is necessary to explore new preparation techniques to produce them in bulk using inexpensive materials to decrease the cost of graphene greatly. Secondly, pristine graphene and GO nanosheets aggregate heavily in water due to large-area π - π interactions and strong Van der Waals interactions between the graphenic layers, which inhibit the material's powerful adsorption capacity[15–17]. Thirdly, because of its small size, it is difficult to separate the powdery material from suspensions in batch process of adsorption. In column mode of adsorption, bed compaction and clogging may occur which can cause problem of disruption of hydraulic flow and pressure head loss.

One promising strategy to overcome these problems is to load graphene and GO nanosheets onto low-cost substrates [16], [18–20][21], which could allow the full expression of the graphene/GO adsorption sites while simultaneously being easily separated from suspensions as well as enable it to be used without any hindrance in column adsorption process. Recently, studies have been conducted on F removal by graphene loaded on many materials such as vegetal activated carbon impregnated with Zr[22], Zr oxide[23], Zirconium-Chitosan/ Graphene Oxide Membrane [24], manganese oxide [25] and basic aluminum sulphate hydrogel [26].

However, these composite graphene-based materials either had low F adsorption capacities or not very inexpensive. Sand is an ideal low-cost framework material for mitigating graphene aggregation because it is an inexpensive and widespread material that can be easily procured.

Zirconium and its complexes have been conventionally used for the colorimetric determination of F due to the high affinity of Zr for F ion[27]. Since F is a hard base and Zr is a hard acid, F forms a stable complex with Zr. Therefore, many studies have used Zr impregnated graphene oxide-loaded adsorbents as useful adsorbent for defluoridation of water[22–24].

There have been few reports of synthesis of graphene-based materials from non-conventional sources[28][29]. The main objective of this study is to develop a highly efficient inexpensive GO-based adsorbent for F management in drinking water. To optimize practical performance of GO materials in F management, GO nanosheets were loaded onto sand particles. The substantial aggregation of GO nanosheets can be easily overcome via coating it on sand particles, which then acts as a framework. The potential adsorption sites concealed in stacked graphene would be exposed in the GO coated sand (GCS), strongly enhancing the adsorption potential of the GO nanosheets.

Extensive use of GO in F adsorption from water would have to overcome the relatively high costs involved in its production. Therefore, in the present work we have synthesized GO from a low-cost material sugar and successfully anchored it on the river sand. Furthermore, Zr was impregnated on to the GCS to enhance its F uptake potential. The nature and morphology of ZIGCS were characterized by Scanning Electron Microscopy (SEM) and Raman spectra analysis. Batch adsorption studies were performed as a function of contact time, initial F concentration, pH and adsorbent dose and the data were fitted to adsorption models. To the best of our knowledge, a nano adsorbent of this kind has not been explored for the defluoridation of water.

2. Materials and methods

2.1. Materials

Common sugar and river sand (~ 0.2 mm particle size) were procured from the local market. Analytical reagent (A.R) grade chemicals, HCl (37 %), H_2SO_4 , NaOH pellets (97 %), ethanol (99.9 %), NaF (99.9%) and ZrOCl_2 (95%) were supplied by Merck, India and used without any further purification. De-ionized water was used for the synthesis of the adsorbent and the adsorption experiments.

2.2. Adsorbent preparation and impregnation

Graphene oxide was anchored on the river sand (GCS) according to the following procedure [28]. Common sugar was used as the precursor for carbon. The sugar used in the experiments was the common table sugar and was obtained from the local market. Table sugar is made up of sucrose. Sucrose is a disaccharide consisting of glucose and fructose. The sugar was dissolved in deionized water. River sand was introduced into the sugar solution such that the sugar to sand ratio was 1:10. The above mixture was dried in hot air oven at 95°C with constant stirring for 6 h to obtain sugar coated sand. The sugar-coated sand mixture was heated in N_2 gas atmosphere by controlling the temperature of furnace in 3 different stages. During the first stage furnace temperature was increased to 200°C with a ramping rate of 3°C per minute. The second stage was to maintain the furnace temperature at 200°C for 1 h. In stage 3, temperature was ramped to 750°C in 1 h of time and the same was maintained for 3 h. The resulting product at the end of stage 3 was graphene oxide coated sand termed as GCS.

2.3. Acid activation of GCS

GCS was further acid activated before impregnating with Zr ions. In a typical procedure, 10 g of Graphene oxide Sand Composite (GCS) was introduced in to a beaker containing 20 mL of concentrated H_2SO_4 . This solution mixture was kept intact for 1 h at room temperature, after which it was filtered and the residue dried at 120°C . The obtained product was termed as acid Activated Graphene oxide Coated Sand (AGCS). The process of acid activation leads to modification of GCS to obtain improved properties of surface area, pore diameters, number of active sites for further reactions[30].

2.4. Zr impregnation of GCS

The AGCS was further impregnated with Zr ions. This was done by stirring AGCS in 5% ZrOCl_2 solution at pH 1.6, at a solution/solid ratio of 4:2 at room temperature (298 K) for 5 days [31]. The impregnated AGCS was filtered and rinsed several times till the effluent was free from Zr and dried at 333 K. The obtained product was termed as Zr impregnated graphene oxide coated sand (ZIGCS). In this process, the AGCS surface with enhanced properties as mentioned above, would ensure uniform coating of its surface with Zr ions. This is an important step as these ions play a significant role in fluoride adsorption process.

2.5.Characterisation of ZIGCS

The as synthesized ZIGCS was characterised by Raman spectra, XPS, SEM and XRD for examining its chemical and physical properties. Raman spectrum was utilized to confirm the graphitic nature of the material anchored on the sand and it was recorded with Raman spectrometer (Horiba Yvoni HR550). Scanning electron microscopy measurements were carried out by using H-7100, HITACHI, Japan, electron microscope operated at 200 KeV. The X-ray photoelectron spectroscopy (XPS) analysis was conducted for elemental analysis of ZIGCS using S-83 probe TM 2803, Fisons instrument with a monochromatic $\text{Al K}\alpha$ x-ray source. The x-ray diffraction data was obtained using PANalytical X'Pert Pro system with Copper $\text{K}\alpha$ as source ($\lambda = 1.5406 \text{ \AA}$) at room temperature.

2.6. Fluoride determination and batch adsorption studies

Fluoride ion concentration in water samples was measured using F ion selective electrode coupled with Orion STAR-A 214 meter by the potentiometric measurement. In order to suppress the interference of other ions present in the solution, TISAB-II (Total Ionic Strength Adjustment Buffer) was added to each sample before making the measurement with the F ion selective electrode. A stock solution of 100 mg F/L was prepared by dissolving 22.1 mg of NaF in 100 mL of deionised water. All the other required concentrations were prepared by serial dilution of the stock solution. In a typical adsorption experiment, 40 mg of adsorbent was added to 20 mL of F solution of 12 mg/L concentration, in a 100-mL capped conical flask. The solution was placed in

a mechanical shaker and agitated with a speed of 200 rpm. The solution was filtered and equilibrium concentration of F ions in aqueous solution was measured after filtration of the suspensions.

The adsorption capacity is expressed as the amount of F ions adsorbed per gram of adsorbent (mg/g) and was calculated as follows:

$$q_e = \left(\frac{C_0 - C_e}{m} \right) V \quad (1)$$

where C_0 and C_e are the initial and equilibrium concentrations of F in the solution (mg/L), respectively, V is the volume of the solution (L) and m is the mass of the adsorbent (g). The percentage adsorption of F ions was calculated using the equation:

$$\text{Adsorption \%} = \frac{C_0 - C_e}{C_0} \times 100 \quad (2)$$

where C_0 and C_e are the initial and equilibrium concentrations of F in solution (mg/L), respectively.

Batches of F adsorption experiments were carried out to optimize various parameters that influence F adsorption such as pH of the solution, contact time, and initial F concentration. Fluoride adsorption capacity of ZIGCS was studied as a function of each parameter at a time, while keeping the other parameters constant. The effect of pH was investigated by adjusting solution pH from 2 to 10, using 0.01 M HCl and 0.01 M NaOH for a solution having an initial F concentration of 12 mg/L with an adsorbent dose of 2 g/L. The influence of contact time on adsorption capacity of ZIGCS, was examined by varying the contact time from 5 min to 100 min, while keeping initial F concentration as 12 mg/L and the adsorbent dose as 2 g/L at pH 4. Adsorption isotherm experiments were performed by varying initial F concentrations from 5 mg/L to 100 mg/L with an adsorbent dosage of 2 g/L at pH 4 taking contact time as 2 h at room temperature. All the experiments were carried out thrice and the mean values of the results were used in data analysis.

2.7. Temperature effect on adsorption

Effect of temperature on defluoridation potential of ZIGCS adsorbent was studied at different initial F concentrations ranging from 10 mg/L to 60 mg/L, adsorbent dose of 2 g/L in 50 mL suspensions at three different temperatures of 303 K, 318 K and 328 K. A temperature-controlled incubator orbital shaker was used to maintain the temperature of the suspensions. Thermodynamic calculations were made on the adsorption data.

2.8. Regeneration and reusability of ZIGCS

Fresh ZIGCS with a dosage of 2 g/L was added to 50 mL F solution of 10 mg/L concentration. Adsorption was carried out for 2 h of contact time at pH 4. After the equilibration, ZIGCS was separated from the aqueous solution, dried and termed as exhausted or F loaded adsorbent. Fluoride loaded ZIGCS was regenerated by desorbing the previously adsorbed F with the use of 0.1 M NaOH as eluent. In a typical regeneration experiment, exhausted adsorbent was soaked in a 0.1 M NaOH solution for 48 h. The adsorbent was then filtered and washed with 0.1 M HCl solution followed by deionized water, dried, and used as the regenerated adsorbent for the next cycle of F adsorption. Five such cycles of adsorption/desorption were conducted.

3. Results and discussion

3.1. Adsorbent characterization

3.1.1. Raman spectra

Raman spectroscopy is a powerful tool for the characterisation of graphene and its derivatives. It is a vibrational spectral technique that is extremely sensitive to geometric structure and bonding within molecules. Even small differences in geometric structure lead to significant differences in the observed Raman spectrum of a molecule. This sensitivity to geometric structure is extremely useful for the study of the different allotropes of carbon (i.e. diamond, carbon nanotubes, fullerenes, carbon nanoribbons, etc.) where the different forms differ only in the relative position of their carbon atoms and the nature of their bonding to one another [32]. Indeed, Raman spectra has evolved as an indispensable tool in laboratories pursuing research in the field of carbon nanomaterials.

Fig 1 shows the Raman spectra of ZIGCS. The confocal Raman spectra obtained was deconvoluted for further analysis. The spectra consist of two major peaks positioned at 1319cm^{-1} and 1604.8cm^{-1} which broadly stands for the D and G band respectively [6,33,34]. The D band indicates the presence of structural disorder in the material [35,36]. The band appearing around 1604.8cm^{-1} in the Raman spectrum is the apparent G band (G_{app}) which is actually a superposition of two bands G and D' . The G band positioned at 1584.9cm^{-1} represents the in-plane vibrational mode involving the sp^2 hybridized carbon atoms that comprises the graphene oxide sheets [22,23]. The additional peak D' at 1605.6cm^{-1} arises due the defects present in the graphitic structure. This could also be due to the presence of many oxygen based functional groups [37]. The presence of G and D bands in the Raman spectra confirms the complete graphitization of the material anchored on the sand as also reported for other graphene-based anchoring materials like activated carbon[36]. The intensity ratio, I_D/I_G , represents the defect density in the material; the value increases with the increase in defects[33,38]. In the current study, I_D/I_G for ZIGCS was calculated to be 1.84. This relatively high value indicates the presence of many defect sites on the material.

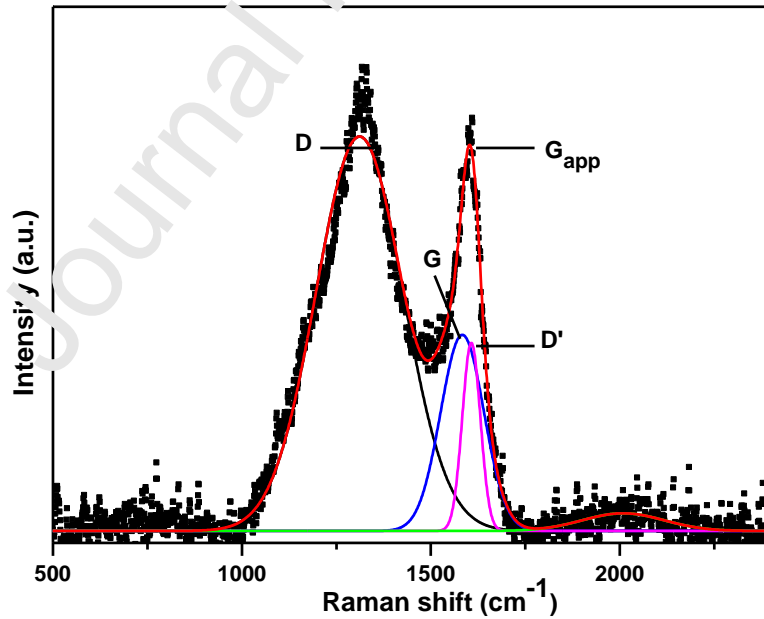


Fig 1: Raman spectra of ZIGCS.

3.1.2 Elemental Analysis using XPS

X-ray Photoelectron Spectroscopy was used to carry out elemental analysis of ZIGCS. As shown in fig 4a, the survey spectrum reveals that the sample is composed only of C, Zr, Si and O which is representative of the sample purity. Fig 2b, 2c and 2d shows the high-resolution spectra of C, Zr and O respectively. The deconvoluted peaks of Carbon shows the peaks at 284.4eV, 285.4eV, 286.7eV, 289.8eV which correspond to the sp^2 hybridised carbon, C – O, C = O, O – C = O respectively. The most significant peak at 284.4 eV corresponds to the non-oxygenated sp^2 hybridised C 1s from the graphene oxide in ZIGCS[28][39]. The other C – O, C = O and O – C = O correspond to the oxygen functionalized carbon atoms of Graphene oxide, which probably act as active sites for fluoride adsorption. As shown in fig 2c, the high resolution spectra of Zr consists of deconvoluted peaks at 182.8 eV and 185.30 eV which correspond to the $3d_{3/2}$ and $3d_{5/2}$ states of Zr which could be attributed to the +4 oxidation state of Zr [40]. This further confirms successful functionalization of the GCS surface with Zirconium ions. The high resolution spectra of Oxygen consists of peaks at 530.4 eV and 531.8eV which could be attributed to C = O, O – C – O; and the one at 532.6 eV correspond to both O = C – O and SiO_2 of sand respectively [41][42,43]. The atomic percentages of the elements present in ZIGCS as obtained from XPS analysis are: C 47.62%, O 40.41%, Zr 1.363% and Si 10.5%.

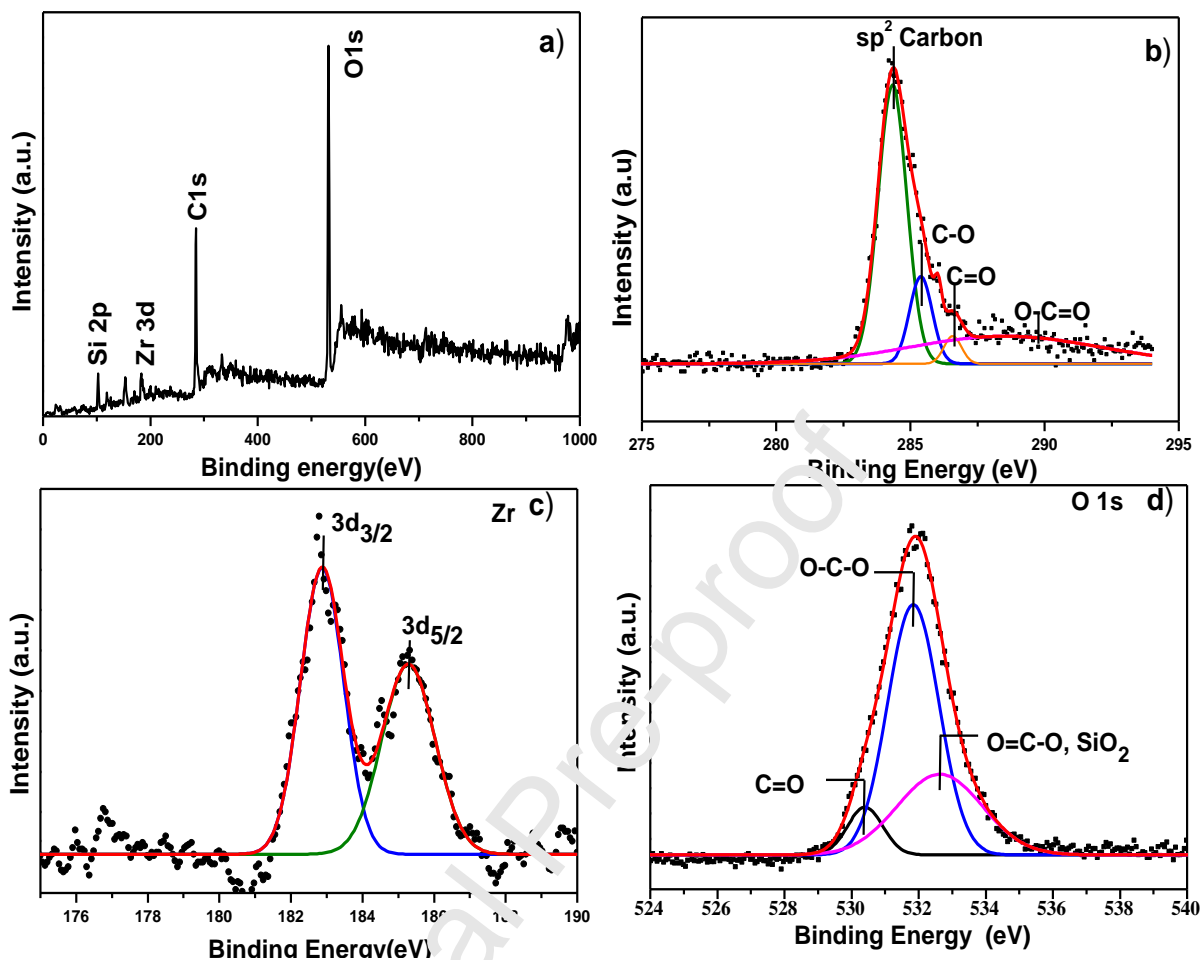


Fig. 2. a) Survey spectrum of ZIGCS, b) High resolution spectra of C, c) High resolution spectra of Zr, d) High resolution spectra of O

Alice A. K. King et. Al [44] in their work reported a metric for distinguishing graphene, graphene oxide and reduced graphene oxide using results obtained from Raman spectra and C/O ratio obtained from elemental analysis. According to this report, Graphene oxide must satisfy the following conditions: as obtained from Raman spectra the difference in peak positions $D' - G_{app}$ must be less than zero; as obtained from elemental analysis of the material, the ratio of C/O must be less than 10. In the present study, the difference $D' - G_{app} = 0.81$, thus satisfying the first condition. Secondly, as obtained from XPS analysis of ZIGCS, the ratio of atomic percentage C/O was calculated to be 1.18. Hence both the mentioned conditions were satisfied, thus

confirming the material to be graphene oxide. The adsorbent is therefore Zr impregnated graphene oxide coated sand.

3.1.3 Surface morphology using SEM

The as synthesised material was characterised using SEM to study the morphology of ZIGCS. The obtained SEM images are shown in Fig 3. A few layers of thin graphene oxide like sheets protruding from the sand surface can be seen in fig 3. This is indicative of the layers of graphene oxide anchored on the sand[25].

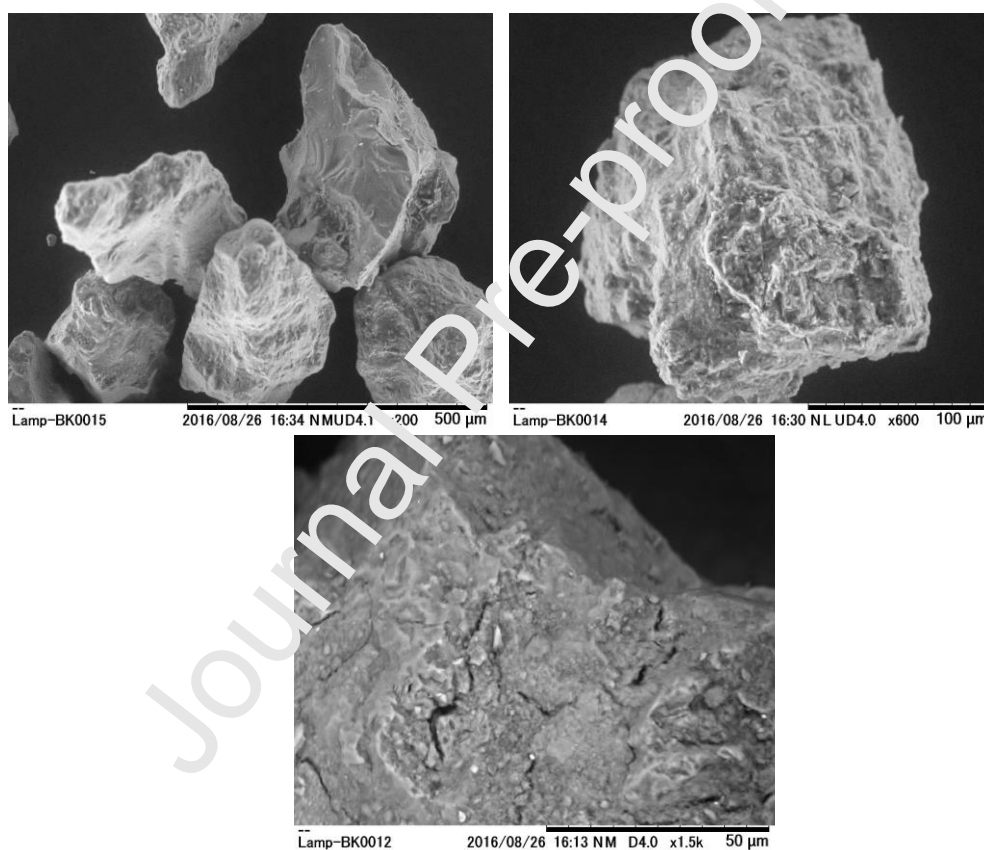


Fig. 3. SEM images of ZIGCS

3.1.4 X-Ray Diffraction

The X-Ray Diffractogram for ZIGCS is shown in Fig. 4. XRD was done for both coated and uncoated sand. The peaks positioned at 2θ values 21.2° , 26.5° , 27.8° , 29.7° , 36.5° , 42.6° correspond to the quartz phase of sand [45,46]. It is noteworthy that the most intense peak corresponds to the sand. The peaks corresponding to the Zirconium impregnated Graphene oxide goes undetected by the XRD technique due to the small thickness of the coat[45].

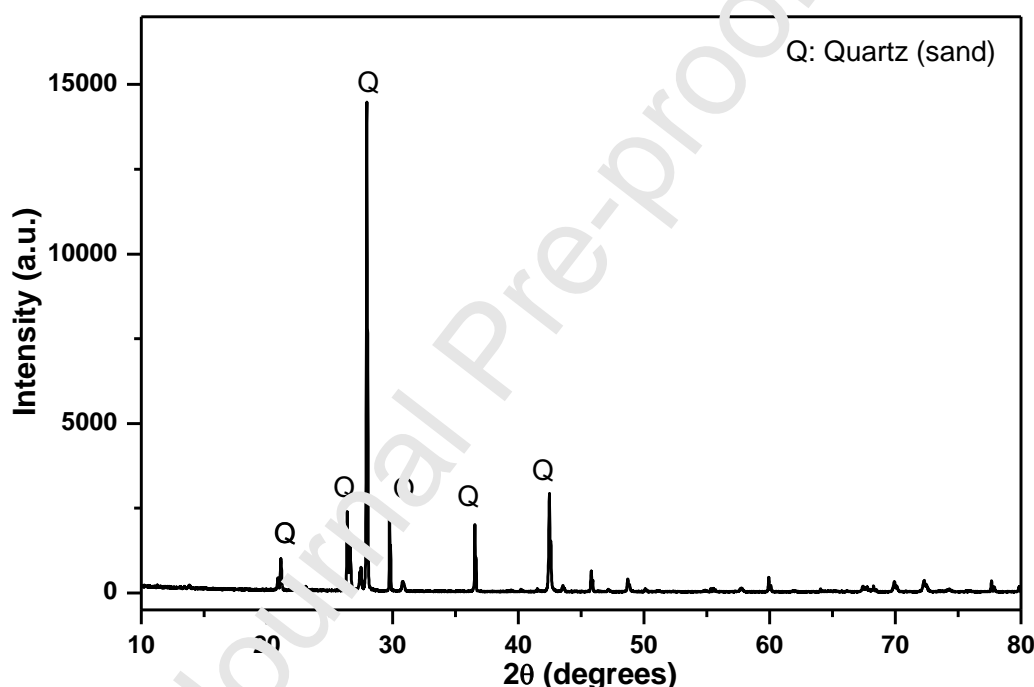


Fig. 4. XRD of ZIGCS

3.2 Fluoride adsorption by GCS, AGCS and ZIGCS

The three graphene-based synthesized materials, GCS, AGCS and ZIGCS were subjected to preliminary F adsorption studies. The results showed that these three materials at a dose of 3 g/L removed 27%, 34%, and 49% of F, respectively from a solution containing 9.6 mg F/g. There was absolutely no fluoride adsorption using the sand as an adsorbent. Hence the adsorption obtained using GCS, AGCS and ZIGCS could be attributed purely to the coated material. The

enhanced F adsorption by ZIGCS might be due to the surface modification of graphene with a strong oxidizing agent which generated more adsorption sites on its surface. Zirconium impregnation results in the formation of a Zr-based Lewis acid sites having hard acid characteristics on the surface of GO through chemisorption process. They might be responsible for the very strong adsorption of Lewis bases of hard base characteristics, such as the F ion [22,23]. The enhanced adsorption capacity of the ZIGCS is probably due to ligand exchange of OH groups attached to the Zr by F and H-bonding between the OH groups on the surface and F ion [23]. Because ZIGCS had the highest F adsorption capacity among the three synthesized materials, this material was used for further adsorption studies.

3.3 Effect of pH on F adsorption by ZIGCS

Solution pH is one of the major influencing parameters in any adsorption process. In the present study, its influence on the F adsorption capacity of ZIGCS was studied by varying the solution pH from 2.0 to 9.0 keeping the other parameters constant (adsorbent dose 2 g/L, initial F concentration 12 mg/L, contact time 2 h, temperature $25 \pm 2^\circ \text{C}$). The results showed that the adsorption increased in acidic medium with maximum of F adsorbed at pH 4 (Fig. 5). However, the adsorbent had adsorption capacity greater than 1 mg/g in the entire pH range 2-8 which is much higher than that of traditional carbon based materials reported earlier [47,48]. This wide pH range window offered by the material enables it to be a potential defluoridation adsorbent for all real-time applications.

The higher F adsorption of ZIGCS in the acidic medium can be explained based on the zero point of charge (pH_{ZPC}) of the adsorbent. The pH_{ZPC} is the pH of an adsorbent suspension at which the net charge on its surface is zero. For a solution of pH less than pH_{ZPC} , the surface has a net positive charge and favours adsorption of anions such as F^- while for a solution pH greater than pH_{ZPC} the surface has a net negative charge and favours cation adsorption. The pH_{ZPC} of ZIGCS was determined by the ΔpH ($\Delta\text{pH} = \text{pH}_f - \text{pH}_i$) method [49]. In a typical experiment, known amount of the ZIGCS was added to the flasks containing double distilled water adjusted to different initial pH values in the range 2-10. The flasks were kept for shaking in a mechanical orbital shaker for 48 h at room temperature. The equilibrium pH of each solution was measured

when the adsorbent was settled. The variation in ΔpH was estimated and plotted against initial and final pH of the solution (Fig 6). These plots showed that ΔpH is zero at $\text{pH} = 4.5$. The ZPC of 4.5 indicates that ZIGCS is positively charged in acidic medium from pH 2 to 4.5 as this pH is less than pH_{ZPC} . Hence the electrostatic attraction favoured the adsorption of F from pH 2 to 4.5. The negative charge on the surface of ZIGCS at pH greater than pH_{ZPC} prevented the electrostatic adsorption of F^- ions, resulting in the decrease of F adsorption capacity at pH greater than pH_{ZPC} .

The F adsorption by ZIGCS as a function of pH shown in Fig 5 is in compliance with the results obtained from pH_{ZPC} measurements of ZIGCS, that F adsorption increased from pH 2 to 4 and then decreased thereafter with further increase of pH up to 9. However, significant quantities of the negatively charged F were also adsorbed at pH above the pH_{ZPC} despite the adsorbent surface had predominantly negative charges. This indicated that F was adsorbed by mechanisms other than electrostatic adsorption such as ligand exchange of F with OH attached to Zr and H-bonding of F with OH group [23]. The decrease in F adsorption with increased pH is also due to increased concentration of OH^- ions that compete with F for adsorption [1]. The reduction of F adsorption at pH 2 compared to that at pH 4 may be due to F forming weakly ionized hydrogen fluoride [1] (HF). As maximum adsorption was observed at pH 4, the remaining adsorption experiments were conducted at pH 4.

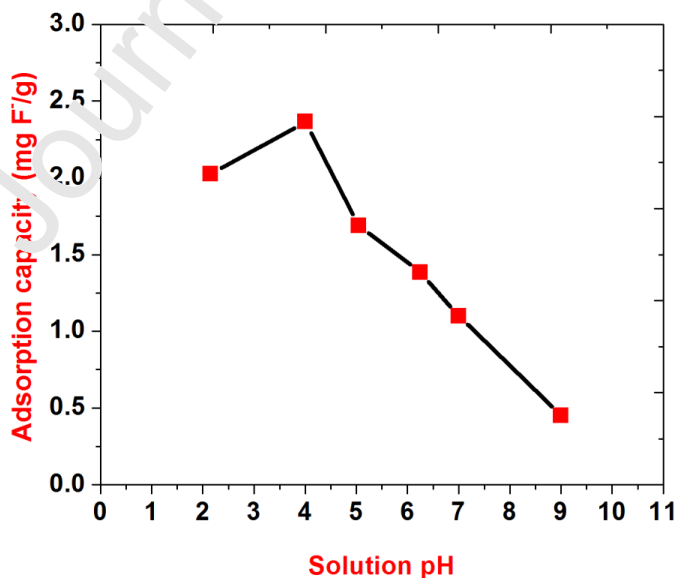


Fig. 5. Influence of pH on F adsorption capacity of ZIGCS

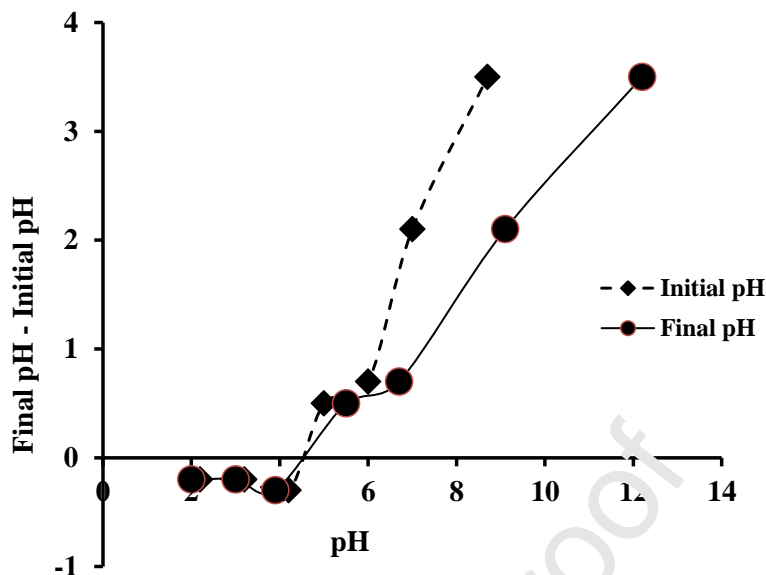


Fig. 6. pH_{zpc} of ZIGCS

3.4 Adsorption kinetics of ZIGCS

The data on the kinetics of F adsorption showed that the adsorption was rapid at the initial stage but took a long time to reach equilibrium (Fig. 7). The fast rate of adsorption was presumably due to the structure of zirconium impregnated graphene oxide anchored on the surface of the sand, which provided plenty of active sites for adsorption of F ions from the aqueous solution with minimum mass transfer resistance. With further increase in time, the reduced availability of the remaining active sites and driving force lowered the adsorption rate and hence equilibrium was reached after a long time.

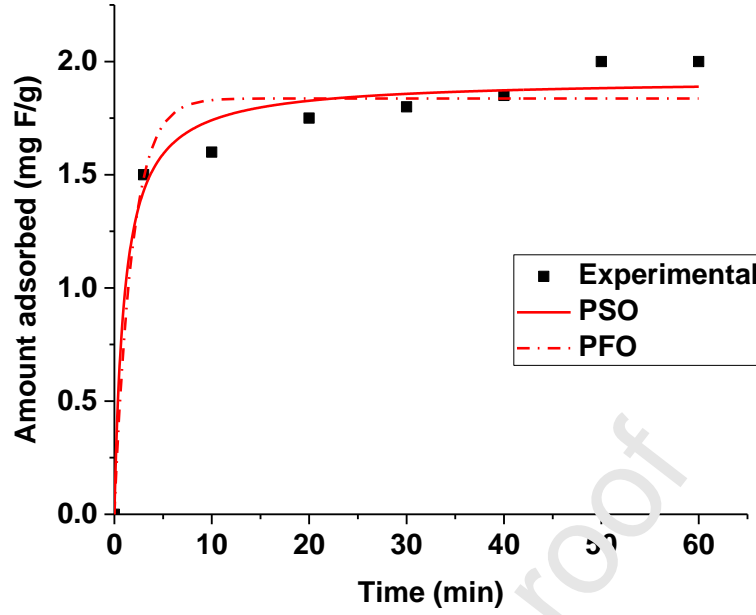


Fig. 7. Effect of contact time on F removal by ZIGCS adsorbent and models' fit to the experimental data (F concentration 12 mg/L, adsorbent dose 2 g/L, pH 4, PFO-pseudo-first order model, PSO-pseudo-second order model).

The data was fitted to the pseudo-first order (equation 3) and pseudo-second order (equation 4) kinetic models represented by the following equations:

$$\frac{dq_t}{dt} = k_1 (q_e - q_t) \quad (3)$$

$$\frac{dq_t}{dt} = k_2 (q_e - q_t)^2 \quad (4)$$

where, q_e = amount of F adsorbed at equilibrium (mg/g)

q_t = amount of F adsorbed at time, t (min) (mg/g) and

k_1 , and k_2 = equilibrium rate constants of pseudo-first order (1/min) and pseudo-second order (g/mg.min) adsorption kinetics, respectively.

The parameters of the kinetic models with statistical evaluation were determined by non-linear regressions using OriginPro software (OriginLab Corporation, USA). The corresponding kinetic parameters and the determination coefficients of the studied models are summarised in Table 1. Pseudo-second order model offered a better fit to the kinetic data with a higher coefficient of determination (R^2) of 0.98 when compared to the pseudo-first order reaction with R^2 value of 0.96. Moreover, the calculated q_e value from the pseudo-second order model was in better agreement with the q_e experimental value. Hence, the pseudo-second order model was a better descriptor of the adsorption kinetics of F by ZIGCS. These results suggested that the overall rate of F adsorption was most likely controlled by a chemical process.

Table 1. Rate constants and coefficients of determination (R^2) of the kinetic models.

$q_{e,exp}$ mg/g	Pseudo-first order parameters			Pseudo-second order parameters		
	k_1 min^{-1}	$q_{e, cal}$ mg/g	R^2	k_2 g/mg min	$q_{e, cal}$ mg/g	R^2
2.0	0.55	1.84	0.96	0.50	1.92	0.98

3.5 Equilibrium adsorption isotherm of ZIGCS

Adsorption isotherms not only describe the interaction of the adsorbate with the adsorbent surface but also quantify the adsorption capacity of an adsorbent. They can be generated based on numerous theoretical models, where the two popular and frequently used models are Langmuir [50] isotherm (equation 5) and Freundlich[51] isotherm (equation 6).

$$q_e = q_{max}bc_e / (1 + bc_e) \quad (5)$$

$$q_e = K_F c_e^{1/n} \quad (6)$$

where q_{max} (mg/g) is the theoretical maximum adsorption capacity of the adsorbent for complete monolayer coverage of F ions, q_e (mg/g) is the equilibrium adsorption capacity, c_e is the equilibrium concentration (mg/L), b (L/mg) is the Langmuir isotherm constant related to

adsorption affinity, K_F is a Freundlich constant related to the adsorption capacity $((\text{mg/g})(\text{L/mg})^{1/n})$ and $1/n$ is another constant inversely related to the adsorption energy between the adsorbent and adsorbate (unit-less) [52]. The parameters of the isotherm models with statistical evaluation were determined by non-linear regressions using OriginPro software (OriginLab Corporation, USA) [22]. The models fit to the experimental data are presented in Fig. 8 and the corresponding parameters including the determination coefficients of the studied models are summarised in Table 2.

In the Langmuir model, the value of the separation factor R_L as calculated from the formula, $R_L = 1 / (1 + bC_m)$ (where C_m is the maximum initial concentration of adsorbate), indicates the favourability of the sorption process, such as unfavourable ($R_L > 1$), favourable ($0 < R_L < 1$) or irreversible ($R_L = 0$) [52]. The calculated R_L values for F adsorption on ZIGCS was 0.25, indicating that the sorption process was favourable.

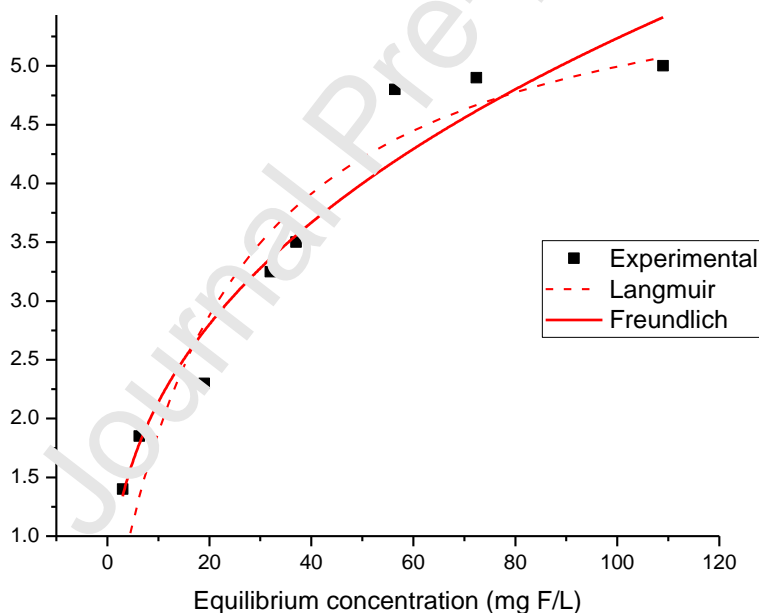


Fig. 8. Equilibrium adsorption isotherm and Langmuir and Freundlich models fit to experimental data of ZIGCS at pH 4.

A χ^2 analysis (equation 7) was conducted to compare the relative suitability of the two models in describing the adsorption data.

$$\chi^2 = \sum \frac{(q_{e,exp} - q_{e,model})^2}{q_{e,model}} \quad (7)$$

where $q_{e, model}$ (mg/g) is equilibrium capacity obtained from the model and $q_{e, exp}$ (mg/g) is the equilibrium adsorption capacity from the experimental data. The smaller the χ^2 value, the higher is the agreement between the calculated adsorption capacity from a model and that obtained from the experimental data. Therefore, a smaller value of χ^2 indicates better suitability of an adsorption model. The χ^2 values estimated for the two studied isotherm models (Table 3) indicate that Freundlich model with higher R^2 value (0.94) had a smaller χ^2 value, thus offered a better fit to the adsorption of F ions by ZIGCS than the Langmuir model. Moreover, the Freundlich characteristic constant n value (2.57), lying in between 1 and 10 indicated a favorable adsorption of F on to ZIGCS. This conveyed the heterogeneous distribution of active sites on the ZIGCS surface and the chemisorption of F ions on to the adsorbent surface. The heterogeneous adsorption sites are probably the graphene oxide and Zr groups in ZIGCS.

Table 2. Langmuir and Freundlich isotherms data of ZIGCS

	Langmuir		Freundlich
q_{max} (mg/g)	6.12	n	2.57
b (L/mg)	0.04	K_F (mg/g) (L/mg) ^{1/n}	0.87
R^2	0.90	R^2	0.94
χ^2	0.35	χ^2	0.18

Although the determination coefficient R^2 (0.90) of the Langmuir model was slightly lower than that of the Freundlich model (Table 2), the Langmuir model can be used to evaluate the monolayer F adsorption capacity of the ZIGCS because of the high R^2 value and this was

found to be 6.12 mg/g, which is one of the highest values previously reported for other carbon-based adsorbents (Table 3). The high adsorption capacity of ZIGCS is mainly due to the contribution of the adsorption capacity of graphene oxide in ZIGCS despite the very large proportion of sand in the material. The amount of Zr impregnated graphene oxide in ZIGCS is 3.5% by weight and the remaining weight percentage is that of sand. Assuming sand has a negligible adsorption of F, a calculation based on this weight percentage shows that the Zr impregnated graphene oxide had very high adsorption capacity of 175 mg/g ($6.12 \times 100/3.5$). Had graphene oxide was used without any supporting material like sand it would not have expressed its high adsorption capacity due to the aggregation of the graphene oxide nanosheets. Li et. al [25] have reported that when graphene oxide was coated on manganese oxide the adsorption capacity increased 8.34 times the adsorption capacity of graphene oxide alone.

Table 3. Comparison of Langmuir maximum F adsorption capacities of different carbon materials

Adsorbent	Maximum F adsorption (mg/g)	Temperature and pH of experiment	Reference
Biomass carbon	3.19	25°C, pH: 5.8	[48]
Pine wood biochar	7.66	25°C, pH: 2.0	[53]
Pine bark biochar	9.77		
Moringa indica based activated carbon	0.23	30°C, pH: 2	[47]
Zirconium impregnated coconut shell carbon	6.4	30°C, pH: 4	[27]
Zirconium impregnated groundnut shell carbon	2.32	30°C, pH: 7	[54]
Zirconium impregnated cashew nut shell carbon	1.23	30°C, pH: 7	[55]
Aluminium impregnated activated carbon	1.07	25°C, pH: 6.2-6.5	[56]
Activated cotton nut shell carbon	1.38-2.47	30°C, pH: 7	[56]
Aligned carbon nanotubes	2.85	30°C, pH: 5	[57]
Graphene oxide loaded onto manganese oxide	11.9	25°C, pH: 6	[25]
Graphene	35.59	25°C, pH: 7	[14]
Zirconium impregnated graphene oxide coated sand (ZIGCS)	6.12	30°C, pH: 4	Present study

Pristine graphene oxide nanosheets aggregate heavily in water due to large-area π - π interactions and strong van der Waals interactions between the graphene oxide layers [10][58], which inhibits the material's powerful adsorption capacity. This stacked aggregation limits access to many potential adsorption sites in the interlayers that are suppressed by confined water between the graphene oxide sheets [59]. The substantial aggregation of graphene oxide

nanosheets has been easily overcome via the coating on sand particles. The potential adsorption sites concealed in stacked graphene oxide might have been exposed in the graphene coated sand (GCS), strongly enhancing the adsorption of the graphene oxide nanosheets. The graphene oxide nanosheets and sand particles produced a synergetic effect in F-removing GCSs, presenting a facile method for large-scale production of graphene oxide -coated materials. Thus, graphene oxide -coated materials using sand particles as a framework are cost-effective and highly efficient adsorbents for removing F from water and will result in enormous opportunities for using novel 2D nanomaterials (graphene-based materials) for environmental applications.

3.6. Effect of temperature and thermodynamics of F adsorption by ZIGCS

The influence of temperature on fluoride adsorption by ZIGCS was studied by varying the temperature from 303 K to 328 K. The equilibrium constants (k_d) of the adsorption process at the three temperatures for the different F concentrations, the ratio of the F concentration in the solid phase (q_e) to that in solution phase (C_e) at equilibrium, were calculated, $\ln(q_e/C_e)$ was plotted against q_e and q_e was extrapolated to zero to obtain k_o (fig 9).

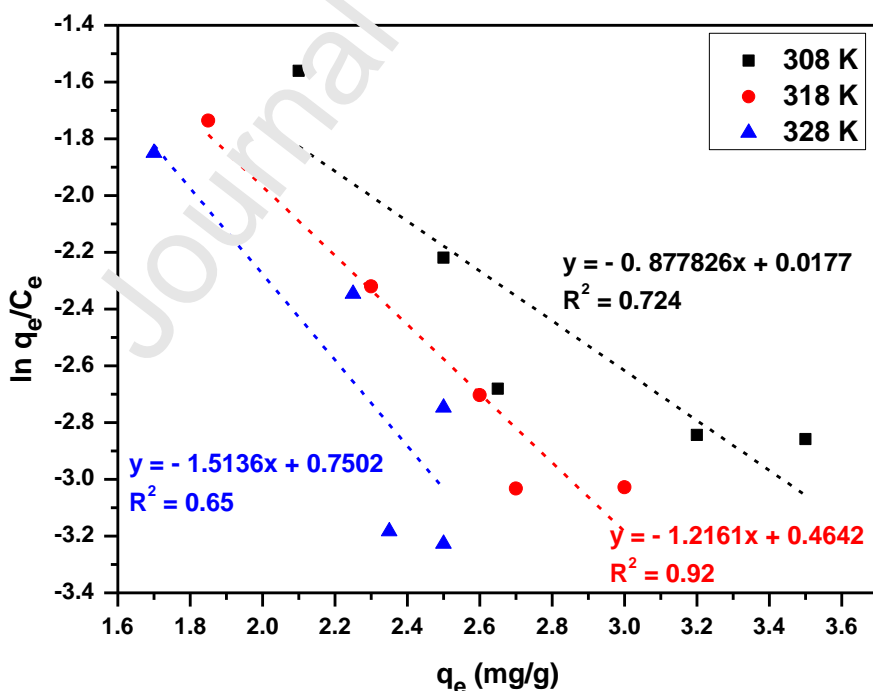


Fig. 9. Relationship of $\ln(q_e/C_e)$ vs q_e at the temperatures of 308 K, 318 K, and 328 K

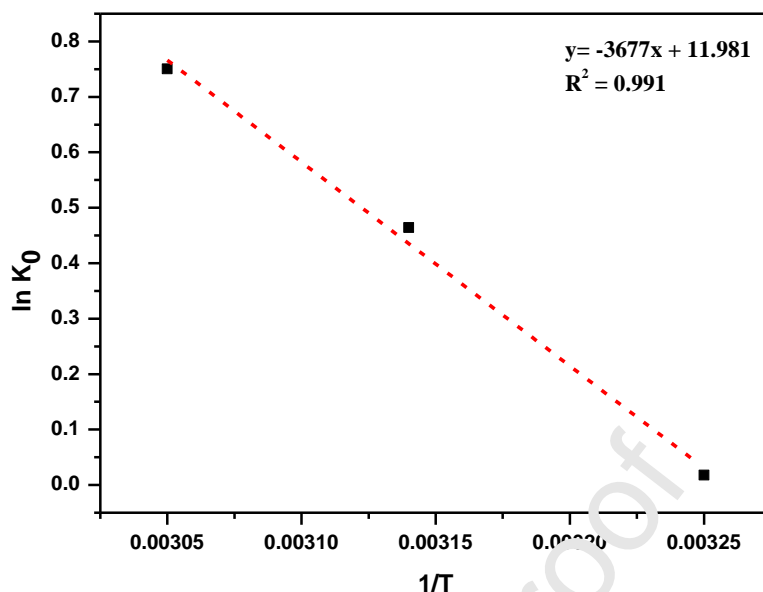


Fig. 10. Relationship of $\ln k_0$ vs $1/T$

The value of k_0 is taken as the thermodynamic equilibrium constant where the concentrations of the adsorbed F and solution F are equal to their respective activities (activity coefficient is one) [25][60,61]. The Gibbs standard free energy change (ΔG°) was calculated using equation (8).

$$\Delta G^\circ = -RT \ln k_0 \quad (8)$$

where T is the absolute temperature and R is the universal gas constant (8.314 J/K.mol). The standard enthalpy change (ΔH°) and standard entropy change (ΔS°) were determined from the slope and intercept of the Van't Hoff plot of $\ln k_0$ vs $1/T$ (fig 10) according to equation (9).

$$\ln k_0 = \Delta S^\circ/R - \Delta H^\circ/RT \quad (9)$$

The ΔG° values (J/mol) obtained for the temperatures of 308 K, 318 K, and 328 K were -45, -1227, and -2045, respectively. The negative ΔG° values indicated thermodynamically feasible and spontaneous nature of the F adsorption by ZIGCS. The increase in negative ΔG° values with increase in temperature suggested a favorable adsorption at high temperatures. The values obtained for ΔH° and ΔS° were 30.6 kJ/mol and 99.6 J/mol.K, respectively. The positive ΔH°

value indicates that the adsorption process was endothermic. As the ΔH° value is greater than 10 kJ/mol the adsorption process is considered to be chemical in nature. Many researchers also have reported endothermic reaction process for the adsorption of F on graphene oxide supported on different materials [23][25][26]. The positive value for the ΔS° obtained in the present study confirmed the affinity of adsorbent for F ions and increase in randomness at the solid/solution interface.

3.7. Regeneration and reusability of ZIGCS

The reusability of an adsorbent mainly depends on the ease with which adsorbate is released from the exhausted adsorbent. Regeneration of an exhausted adsorbent is an important factor which decides the cost effectiveness of the adsorption process. In this study, the regenerated adsorbent was reused for F adsorption by treating a F concentration of 10 mg/L at an adsorbent dose of 2 g/L. The F removal was found to be 75% during the initial adsorption process. The exhausted adsorbent was regenerated and subjected to adsorption studies for five repeated adsorption/desorption cycles. Percent F adsorption was estimated after each recycle and results are presented in Fig 11. It was observed that the F removal efficiency of the recycled ZIGCS remained high at a value of nearly 57% even after 5 regeneration cycles. This is approximately equal to 75% of the initial adsorption capacity. Higher degree of F adsorption capacity reduction was reported for many other adsorbents. For example, F adsorption capacity decreased from 90% to 60% after four cycles of regenerations of Zr oxide/graphene oxide composite adsorbent [23] and from 90% to 50% after four cycles of regenerations of graphene oxide/alginate hybrid biopolymeric beads [62]. The results indicated that ZIGCS could be satisfactorily regenerated and reused to treat F contaminated water.

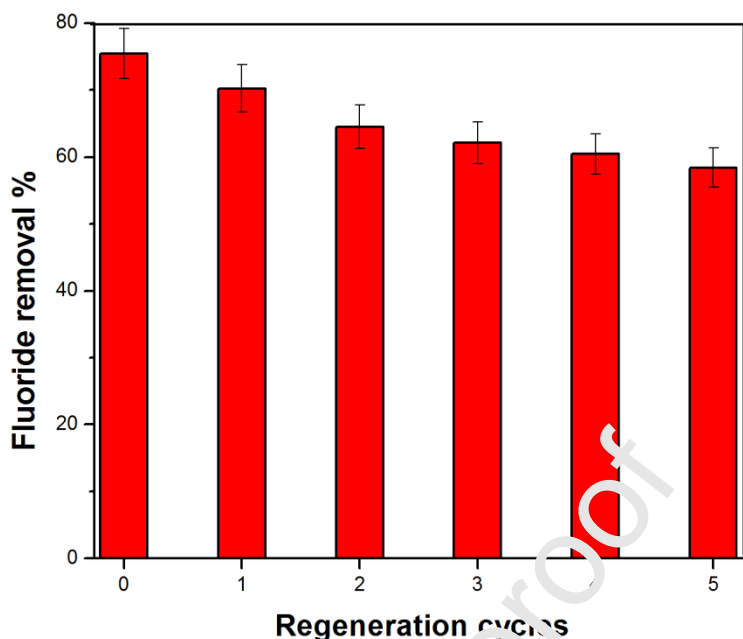


Fig. 11. Percent F removal by adsorption on to ZIGCS from a solution containing 10 mg F/L at ZIGCS dose of 2 g/L after each of five adsorption/desorption cycles.

4 Conclusions:

The adsorbent, graphene oxide coated sand was produced from very inexpensive materials, sugar and river sand. The maximum Langmuir monolayer adsorption capacity of ZIGCS was found to be 6.12 mgF/g which is one of the highest among the other carbon adsorbents used for defluoridation. Assuming that the sand in ZIGCS (97% by weight) has a negligible adsorption of F, it is estimated that the Zr impregnated graphene oxide alone (3%) had a very high adsorption capacity of 175 mg F/g. However, graphene oxide alone cannot be used as adsorbent because of the substantial aggregation of graphene oxide nanosheets in water losing its high adsorption capacity. This aggregation has been easily overcome via the coating on sand particles which provided a cost-effective framework for the graphene oxide. The adsorption of F on to ZIGCS was found to be pH dependent and exhibited considerable F adsorption, for the entire pH range of 2-9 with maximum adsorption at pH 4, close to its ZPC of 4.5. This wide range pH window offered by the material enabled it to be a potential defluoridation adsorbent for all real-time applications. The kinetics of adsorption was very rapid initially adsorbing >80% F within few minutes due to the special one-atom-thick layered structure of graphene oxide anchored on the

surface of the sand. The equilibrium isotherm data fitted well with Freundlich model and the kinetic data was successfully described by pseudo-second order kinetic model. The F removal efficiency by recycled ZIGCS was nearly 75% of the original value even after 5 regeneration cycles indicating that ZIGCS could be regenerated and reused to treat F contaminated water, thus reducing the cost of the treatment process. The very rapid kinetics of adsorption, considerable high adsorption capacity, repeated usability, green methodology of synthesis and the availability of the materials across the world enables ZIGCS to be a viable economical material for providing a solution for commercially feasible nano material- based F water filter.

Financial Support

This research work was supported by Kurita Asia Research Grant (grant no. 19P010) provided by Kurita water and Environment Foundation (KWEF), Japan

5 Acknowledgements

The authors are grateful to Japan advanced Institute of Science and Technology (JAIST), Ishikawa, Japan for lending the XPS facility.

6 References

- [1] P. Loganathan, S. Vigneswaran, J. Kandasamy, R. Naidu, Defluoridation of drinking water using adsorption processes, *J. Hazard. Mater.* 248–249 (2013) 1–19. <https://doi.org/10.1016/j.jhazmat.2012.12.043>.
- [2] M.R. Khairnar, A.S. Dodamani, H.C. Jadhav, R.G. Naik, M.A. Deshmukh, Mitigation of fluorosis - A review, *J. Clin. Diagnostic Res.* 9 (2015) ZE05–ZE09. <https://doi.org/10.7860/JCDR/2015/13261.6085>.
- [3] J.J Murray, *Appropriate use of Fluoride for Human Health*, W.H.O Organization, 1986.
- [4] S.M. Maliyekkal, T.S. Sreeprasad, D. Krishnan, S. Kouser, A.K. Mishra, U. V. Waghmare, T. Pradeep, Graphene: A reusable substrate for unprecedented adsorption of pesticides, *Small.* 9 (2013) 273–283. <https://doi.org/10.1002/smll.201201125>.

- [5] S. Charleston, T.K. River, Activated Carbon Used for, 1 (1967) 287–291.
- [6] S.K. Yadav, R. Kumar, A.K. Sundramoorthy, R.K. Singh, C.M. Koo, Simultaneous reduction and covalent grafting of polythiophene on graphene oxide sheets for excellent capacitance retention, RSC Adv. 6 (2016) 52945–52949.
<https://doi.org/10.1039/c6ra07904k>.
- [7] A.T. Smith, A.M. LaChance, S. Zeng, B. Liu, L. Sun, Synthesis, properties, and applications of graphene oxide/reduced graphene oxide and their nanocomposites, Nano Mater. Sci. 1 (2019) 31–47. <https://doi.org/10.1016/j.nanoms.2019.02.004>.
- [8] L. Sun, Structure and synthesis of graphene oxide, Chinese J. Chem. Eng. 27 (2019) 2251–2260. <https://doi.org/10.1016/j.cjche.2019.05.003>.
- [9] R. Kumar, R.K. Singh, A.R. Vaz, R. Savu, S.A. Moshkalev, Self-Assembled and One-Step Synthesis of Interconnected 3D Network of Fe₃O₄/Reduced Graphene Oxide Nanosheets Hybrid for High-Performance Supercapacitor Electrode, ACS Appl. Mater. Interfaces. 9 (2017) 8880–8890. <https://doi.org/10.1021/acsami.6b14704>.
- [10] V. Georgakilas, M. Otyepka, A.P. Bourlinos, V. Chandra, N. Kim, K.C. Kemp, P. Hobza, R. Zboril, K.S. Kim, Functionalization of graphene: Covalent and non-covalent approach, Chem. Rev. 112 (2012) 6156–6214. <https://doi.org/10.1021/cr3000412>.
- [11] S.K. Tiwari, S. Saloo, N. Wang, A. Huczko, Graphene research and their outputs: Status and prospect, J. Sci. Adv. Mater. Devices. 5 (2020) 10–29.
<https://doi.org/10.1016/j.jsamd.2020.01.006>.
- [12] and R.S.R. Meryl D. Stoller, Sungjin Park, Yanwu Zhu, Jinho An, Graphene-Based Ultracapacitors, NANO Lett. 8 (2008) 3498–3502.
<https://doi.org/10.1021/acs.langmuir.6b03602>.
- [13] S. Zhang, H. Wang, J. Liu, C. Bao, Measuring the specific surface area of monolayer graphene oxide in water, Mater. Lett. 261 (2020) 127098.
<https://doi.org/10.1016/j.matlet.2019.127098>.

- [14] Y. Li, P. Zhang, Q. Du, X. Peng, T. Liu, Z. Wang, Y. Xia, W. Zhang, K. Wang, H. Zhu, D. Wu, Adsorption of fluoride from aqueous solution by graphene, *J. Colloid Interface Sci.* 363 (2011) 348–354. <https://doi.org/10.1016/j.jcis.2011.07.032>.
- [15] G. Zhao, L. Jiang, Y. He, J. Li, H. Dong, X. Wang, W. Hu, Sulfonated graphene for persistent aromatic pollutant management, *Adv. Mater.* 23 (2011) 3959–3963. <https://doi.org/10.1002/adma.201101007>.
- [16] X. Liu, H. Zhang, Y. Ma, X. Wu, L. Meng, Y. Guo, G. Yu, Y. Liu, Graphene-coated silica as a highly efficient sorbent for residual organophosphorus pesticides in water, *J. Mater. Chem. A*. 1 (2013) 1875–1884. <https://doi.org/10.1039/c2ta00173j>.
- [17] J. Zhao, Z. Wang, Q. Zhao, B. Xing, Adsorption of phenanthrene on multilayer graphene as affected by surfactant and exfoliation, *Environ. Sci. Technol.* 48 (2014) 331–339. <https://doi.org/10.1021/es403873r>.
- [18] Y. Sun, S. Yang, G. Zhao, Q. Wang, X. Wang, Adsorption of polycyclic aromatic hydrocarbons on graphene oxides and reduced graphene oxides, *Chem. - An Asian J.* 8 (2013) 2755–2761. <https://doi.org/10.1002/asia.201300496>.
- [19] A.F.M. Ibrahim, Y.S. Lin, Synthesis of graphene oxide membranes on polyester substrate by spray coating for gas separation, *Chem. Eng. Sci.* 190 (2018) 312–319. <https://doi.org/10.1016/j.ces.2018.06.031>.
- [20] R. Alrammouz, J. Podlecki, A. Vena, R. Garcia, P. Abboud, R. Habchi, B. Sorli, Highly porous and flexible capacitive humidity sensor based on self-assembled graphene oxide sheets on a paper substrate, *Sensors Actuators, B Chem.* 298 (2019) 126892. <https://doi.org/10.1016/j.snb.2019.126892>.
- [21] K. Yu, P. Shao, P. Meng, T. Chen, J. Lei, X. Yu, R. He, F. Yang, W. Zhu, T. Duan, Superhydrophilic and highly elastic monolithic sponge for efficient solar-driven radioactive wastewater treatment under one sun, *J. Hazard. Mater.* 392 (2020) 122350. <https://doi.org/10.1016/j.jhazmat.2020.122350>.

- [22] P. Marin, A.N. Módenes, R. Bergamasco, P.R. Paraíso, S. Hamoudi, Synthesis, Characterization and Application of ZrCl₄-Graphene Composite Supported on Activated Carbon for Efficient Removal of Fluoride to Obtain Drinking Water, *Water. Air. Soil Pollut.* 227 (2016). <https://doi.org/10.1007/s11270-016-3188-1>.
- [23] S. Mohan, V. Kumar, D.K. Singh, S.H. Hasan, Synthesis and characterization of rGO/ZrO₂ nanocomposite for enhanced removal of fluoride from water: Kinetics, isotherm, and thermodynamic modeling and its adsorption mechanism, *RSC Adv.* 6 (2016) 87523–87538. <https://doi.org/10.1039/c6ra15460c>.
- [24] J. Zhang, N. Chen, P. Su, M. Li, C. Feng, Fluoride removal from aqueous solution by Zirconium-Chitosan/Graphene Oxide Membrane, *React. Funct. Polym.* 114 (2017) 127–135. <https://doi.org/10.1016/j.reactfunctpolym.2017.03.008>.
- [25] Y. Li, Q. Du, J. Wang, T. Liu, J. Sun, Y. Wang, Z. Wang, Y. Xia, L. Xia, Defluoridation from aqueous solution by manganese oxide coated graphene oxide, *J. Fluor. Chem.* 148 (2013) 67–73. <https://doi.org/10.1016/j.jfluchem.2013.01.028>.
- [26] Y. Chen, Q. Zhang, L. Chen, H. Bai, L. Li, Basic aluminum sulfate@graphene hydrogel composites: Preparation and application for removal of fluoride, *J. Mater. Chem. A* 1 (2013) 13101–13110. <https://doi.org/10.1039/c3ta13285d>.
- [27] R.S. Sathish, N.S.R. Raju, G.S. Raju, G.N. Rao, K.A. Kumar, C. Janardhana, Equilibrium and kinetic studies for fluoride adsorption from water on zirconium impregnated coconut shell carbon, *Sep. Sci. Technol.* 42 (2007) 769–788. <https://doi.org/10.1080/01496390601070067>.
- [28] S. Sen Gupta, T.S. Sreeprasad, S.M. Maliyekkal, S.K. Das, T. Pradeep, Graphene from sugar and its application in water purification, *ACS Appl. Mater. Interfaces* 4 (2012) 4156–4163. <https://doi.org/10.1021/am300889u>.
- [29] R. Kumar, E. Joanni, R.K. Singh, D.P. Singh, S.A. Moshkalev, Recent advances in the synthesis and modification of carbon-based 2D materials for application in energy

- conversion and storage, *Prog. Energy Combust. Sci.* 67 (2018) 115–157.
<https://doi.org/10.1016/j.pecs.2018.03.001>.
- [30] D.K. Dutta, *Clay mineral catalysts*, 1st ed., Elsevier Ltd., 2018.
<https://doi.org/10.1016/B978-0-08-102432-4.00009-3>.
- [31] R.S. Sathish, S. Sairam, V.G. Raja, G.N. Rao, C. Janardhana, Defluoridation of water using zirconium impregnated coconut fiber carbon, *Sep. Sci. Technol.* 43 (2008) 3676–3694. <https://doi.org/10.1080/01496390802222541>.
- [32] M.S. Dresselhaus, A. Jorio, M. Hofmann, G. Dresselhaus, R. Naito, Perspectives on carbon nanotubes and graphene Raman spectroscopy, *Nano Lett.* 10 (2010) 751–758.
<https://doi.org/10.1021/nl904286r>.
- [33] R. Kumar, E. Joanni, R. Savu, M.S. Pereira, R.K. Singh, C.J.L. Constantino, L.T. Kubota, A. Matsuda, S.A. Moshkalev, Fabrication and electrochemical evaluation of micro-supercapacitors prepared by direct laser writing on free-standing graphite oxide paper, *Energy*. 179 (2019) 676–684. <https://doi.org/10.1016/j.energy.2019.05.032>.
- [34] R. Kumar, R. Matsuo, K. Kishida, M.M. Abdel-Galeil, Y. Suda, A. Matsuda, Homogeneous reduced graphene oxide supported NiO-MnO₂ ternary hybrids for electrode material with improved capacitive performance, *Electrochim. Acta*. 303 (2019) 246–256. <https://doi.org/10.1016/j.electacta.2019.02.084>.
- [35] K.P. Loh, Q. Bao, P.K. Ang, J. Yang, The chemistry of graphene, *J. Mater. Chem.* 20 (2010) 2277–2289. <https://doi.org/10.1039/b920539j>.
- [36] F. Yu, J. Ma, S. Han, Adsorption of tetracycline from aqueous solutions onto multi-walled carbon nanotubes with different oxygen contents, *Sci. Rep.* 4 (2014) 1–8.
<https://doi.org/10.1038/srep05326>.
- [37] S. Jaworski, M. Wierzbicki, E. Sawosz, A. Jung, G. Gielerak, J. Biernat, H. Jaremek, W. Łojkowski, B. Woźniak, J. Wojnarowicz, L. Stobiński, A. Małolepszy, M. Mazurkiewicz-Pawlicka, M. Łojkowski, N. Kurantowicz, A. Chwalibog, Graphene oxide-based

- nanocomposites decorated with silver nanoparticles as an antibacterial agent, *Nanoscale Res. Lett.* 13 (2018). <https://doi.org/10.1186/s11671-018-2533-2>.
- [38] I.S. El-Hallag, M.N. El-Nahass, S.M. Youssry, R. Kumar, M.M. Abdel-Galeil, A. Matsuda, Facile in-situ simultaneous electrochemical reduction and deposition of reduced graphene oxide embedded palladium nanoparticles as high performance electrode materials for supercapacitor with excellent rate capability, *Electrochim. Acta.* 314 (2019) 124–134. <https://doi.org/10.1016/j.electacta.2019.05.065>.
- [39] F.T. Johra, J.W. Lee, W.G. Jung, Facile and safe graphene preparation on solution based platform, *J. Ind. Eng. Chem.* 20 (2014) 2883–2887. <https://doi.org/10.1016/j.jiec.2013.11.022>.
- [40] X. Dou, D. Mohan, C.U. Pittman, S. Yang, Remediating fluoride from water using hydrous zirconium oxide, *Chem. Eng. J.* 199–200 (2012) 236–245. <https://doi.org/10.1016/j.cej.2012.05.084>.
- [41] S. Qiu, X. Ren, X. Zhou, T. Zhang, L. Cong, Y. Hu, Nacre-Inspired Black Phosphorus/Nanofibrillar Cellulose Composite Film with Enhanced Mechanical Properties and Superior Fire Resistance, *ACS Appl. Mater. Interfaces.* (2020). <https://doi.org/10.1021/acsaami.0c09685>.
- [42] J. Lei, H. Liu, D. Yin, L. Zhou, J.A. Liu, Q. Chen, X. Cui, R. He, T. Duan, W. Zhu, Boosting the Loading of Metal Single Atoms via a Bioconcentration Strategy, *Small.* 16 (2020) 1–10. <https://doi.org/10.1002/smll.201905920>.
- [43] J. Lei, Q. Guo, D. Yin, X. Cui, R. He, T. Duan, W. Zhu, Bioconcentration and bioassembly of N/S co-doped carbon with excellent stability for supercapacitors, *Appl. Surf. Sci.* 488 (2019) 316–325. <https://doi.org/10.1016/j.apsusc.2019.05.136>.
- [44] A.A.K. King, B.R. Davies, N. Noorbehesht, P. Newman, T.L. Church, A.T. Harris, J.M. Razal, A.I. Minett, A new raman metric for the characterisation of graphene oxide and its derivatives, *Sci. Rep.* 6 (2016) 1–6. <https://doi.org/10.1038/srep19491>.

- [45] S.A. Chaudhry, T.A. Khan, I. Ali, Zirconium oxide-coated sand based batch and column adsorptive removal of arsenic from water: Isotherm, kinetic and thermodynamic studies, *Egypt. J. Pet.* 26 (2017) 553–563. <https://doi.org/10.1016/j.ejpe.2016.11.006>.
- [46] S.A. Abo-El-Enein, A.H. Ali, F.N. Talkhan, H.A. Abdel-Gawwad, Application of microbial biocementation to improve the physico-mechanical properties of cement mortar, *HBRC J.* 9 (2013) 36–40. <https://doi.org/10.1016/j.hbrj.2012.10.004>.
- [47] S.I.S. Karthikeyan G., Fluoridesorption using MORRINGA INDICA based activated carbon, *J. Environ. Heal. Sci. Eng. Eng.* 4 (2007) 21–28.
- [48] S. Sinha, K. Pandey, D. Mohan, K.P. Singh, Removal of fluoride from Aqueous Solutions by Eichhornia crassipes Biomass and Its Carbonized Form, *Ind. Eng. Chem. Res.* 42 (2003) 6911–6918. <https://doi.org/10.1021/ie030544k>.
- [49] T. Nur, P. Loganathan, T.C. Nguyen, S. Vigneswaran, G. Singh, J. Kandasamy, Batch and column adsorption and desorption of fluoride using hydrous ferric oxide: Solution chemistry and modeling, *Chem. Eng. J.* 247 (2014) 93–102. <https://doi.org/10.1016/j.cej.2014.03.009>.
- [50] Langmuir Irving, The Adsorption of Gases on Plane Surfaces of Mica, *J. Am. Chem. Soc.* 60 (1938) 467–475. <https://doi.org/10.1021/ja01269a066>.
- [51] H. Freundlich, Over the Adsorption in Solution, *J. Phys. Chem.* 57 (1906) 385–471. <https://doi.org/10.1515/zpch-1907-5723>.
- [52] G. Naidu, T. Nur, P. Loganathan, J. Kandasamy, S. Vigneswaran, Selective sorption of rubidium by potassium cobalt hexacyanoferrate, 2016. <https://doi.org/10.1016/j.seppur.2016.03.001>.
- [53] D. Mohan, R. Sharma, V.K. Singh, P. Steele, C.U. Pittman, Fluoride removal from water using bio-char, a green waste, low-cost adsorbent: Equilibrium uptake and sorption dynamics modeling, *Ind. Eng. Chem. Res.* 51 (2012) 900–914. <https://doi.org/10.1021/ie202189v>.

- [54] G. Alagumuthu, M. Rajan, Kinetic and equilibrium studies on fluoride removal by zirconium (iv)-impregnated groundnut shell carbon, *Hem. Ind.* 64 (2010) 295–304. <https://doi.org/10.2298/HEMIND100307017A>.
- [55] G. Alagumuthu, M. Rajan, Equilibrium and kinetics of adsorption of fluoride onto zirconium impregnated cashew nut shell carbon, *Chem. Eng. J.* 158 (2010) 451–457. <https://doi.org/10.1016/j.cej.2010.01.017>.
- [56] R. Leyva Ramos, J. Ovalle-Turrubiarres, M.A. Sanchez-Castillo, Adsorption of fluoride from aqueous solution on aluminum-impregnated carbon, *Carbon N. Y.* 37 (1999) 609–617. [https://doi.org/10.1016/S0008-6223\(98\)00231-0](https://doi.org/10.1016/S0008-6223(98)00231-0).
- [57] P. Taylor, Y.H. Li, S. Wang, X. Zhang, J. Wei, C. Xu, Z. Luan, D. Wu, B. Wei, Removal of fluoride from water by carbon nanotube supported alumina, (2008) 37–41.
- [58] J. Wang, Z. Chen, B. Chen, Adsorption of polycyclic aromatic hydrocarbons by graphene and graphene oxide nanosheets, *Environ. Sci. Technol.* 48 (2014) 4817–4825. <https://doi.org/10.1021/es405227u>.
- [59] G. Cicero, J.C. Grossman, E. Schwab, F. Gygi, G. Galli, Water confined in nanotubes and between graphene sheets: A first principle study, *J. Am. Chem. Soc.* 130 (2008) 1871–1878. <https://doi.org/10.1021/ja074418+>.
- [60] A.A. Khan, R.P. Singh, Adsorption thermodynamics of carbofuran on Sn (IV) arsenosilicate in H^+ , Na^+ and Ca^{2+} forms, *Colloids and Surfaces.* 24 (1987) 33–42. [https://doi.org/10.1016/0166-6622\(87\)80259-7](https://doi.org/10.1016/0166-6622(87)80259-7).
- [61] S.I. Lyubchik, A.I. Lyubchik, O.L. Galushko, L.P. Tikhonova, J. Vital, I.M. Fonseca, S.B. Lyubchik, Kinetics and thermodynamics of the Cr(III) adsorption on the activated carbon from co-mingled wastes, *Colloids Surfaces A Physicochem. Eng. Asp.* 242 (2004) 151–158. <https://doi.org/10.1016/j.colsurfa.2004.04.066>.
- [62] F.T. Johra, J. Lee, W. Jung, Facile and safe graphene preparation on solution based platform *Journal of Industrial and Engineering Chemistry Facile and safe graphene*

preparation on solution based platform, J. Ind. Eng. Chem. 20 (2014) 2883–2887.
<https://doi.org/10.1016/j.jiec.2013.11.022>.

List of Figures

Fig 1: Raman spectra of ZIGCS.

Fig. 2. a) Survey spectrum of ZIGCS, b) High resolution spectra of C, c) High resolution spectra of Zr, d) High resolution spectra of O

Fig. 3. SEM images of ZIGCS

Fig. 4. XRD of ZIGCS

Fig. 5. Influence of pH on F adsorption capacity of ZIGCS

Fig. 6. pH_{zpc} of ZIGCS.

Fig. 7. Effect of contact time on F removal by ZIGCS adsorbent and models' fit to the experimental data (F concentration 12 mg/L, adsorbent dose 2 g/L, pH 4, PFO-pseudo-first order model, PSO-pseudo-second order model).

Fig. 8. Equilibrium adsorption isotherm and Langmuir and Freundlich models fit to experimental data of ZIGCS at pH 4.

Fig. 9. Relationship of $\ln(q_e/c_e)$ vs q_e at the temperatures of 308 K, 318 K, and 328 K

Fig. 10. Relationship of $\ln k_0$ vs $1/T$

Fig. 11. Percent F removal by adsorption on to ZIGCS from a solution containing 10 mg F/L at a ZIGCS dose of 2 g/L after each of five adsorption/desorption cycles.

List of Tables

Table 1. Rate constants and coefficients of determination (R^2) of the kinetic models.

Table 2. Langmuir and Freundlich isotherms data of ZIGCS

Table 3. Comparison of Langmuir maximum F adsorption capacities of different carbon materials

Journal Pre-proof

Author Statement

CRedit roles:

C. Prathibha: Conceptualization, Methodology, Funding acquisition; Investigation; Project administration; Resources and Writing- Original draft preparation

Anjana Biswas: Data analysis and editing

Paripurnanda Loganathan: Reviewing and Editing

Mahatheva Kalaruban: Software

L. A. Avinash Chunduri: Methodology and Data curation

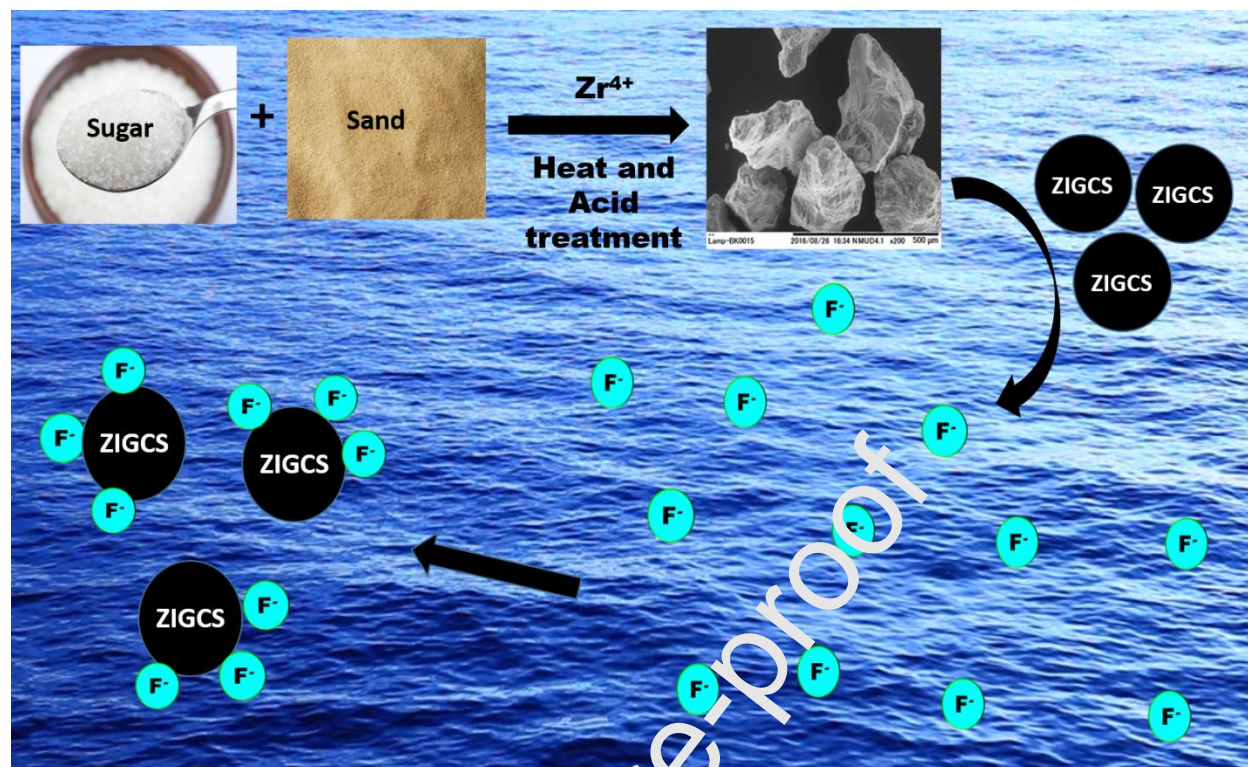
Shiva Konda Reddy: Data curation

Kamisetti Venkatarmaniah: Validation, Reviewing and Editing

Declaration of competing interest

The authors declare that they have no known competing financial interests or personal relationships that could have appeared to influence the work reported in this paper.

Journal Pre-proof



Graphical abstract

Highlights

1. ZIGCS, a product of Zirconium Impregnated Graphene oxide, anchored on Sand is a low cost adsorbent for defluoridation of water
2. The adsorbent is produced from inexpensive materials: table sugar and sand
3. Quick and rapid Removal of fluoride is possible with ZIGCS
4. It could retain 75% of its F^- removal capacity even after five regeneration cycles